Chaotic nature of turbulent Bose-Einstein condensates

P. E. S. Tavares,[1,*] A. R. Fritsch,[1] G. D. Telles,[1] M. S. Hussein,[2,3,4] F. Impens,[5] R. Kaiser,[6] and V. S. Bagnato[1]

[1] *Instituto de Física de São Carlos, Universidade de São Paulo, Caixa Postal 369, 13560-970 São Carlos, SP, Brazil*
[2] *Instituto de Estudos Avançados, Universidade de São Paulo, Caixa Postal 72012, 05508-970 São Paulo, SP, Brazil*
[3] *Instituto de Física, Universidade de São Paulo, Caixa Postal 66318, 05314-970 São Paulo, SP, Brazil*
[4] *Departamento de Física, Instituto Tecnológico de Aeronaútica, DCTA, 12.228-900 São José dos Campos, SP, Brazil*
[5] *Instituto de Física, Universidade Federal do Rio de Janeiro, Caixa Postal 68528, 21941-972 Rio de Janeiro, RJ, Brazil*
[6] *Université Nice Sophia Antipolis, Institut Non-Linéaire de Nice, CNRS UMR 7335, F-06560 Valbonne, France*

(Dated: September 26, 2016)

We report a detailed analysis of the chaotic nature of Quantum Turbulence through a judicial examination of the 2nd order density-density correlation function. We find the almost identical behavior of the average density of the turbulent condensate as compared to that of the regular condensate. The cause of the chaos was traced to the vortices as the correlation length was found to be close to the size of a single vortex. We further make the observation of a similarity between the dynamics of a freely expanding turbulent Bose-Einstein condensate and the propagation of an optical speckle pattern. Both follow very similar basic propagation characteristics. The second-order intensity-intensity correlation function is calculated for the speckle light and the correlation lengths of the two phenomena are used to substantiate the aforementioned similarity.

Since the advent of coherent matter wave sources, as a Bose-Einstein condensate (BEC) or an atom laser, atom optics become an important research field. The free-propagation of coherent atomic waves has been the object of various theoretical [1–3] and experimental studies [4–7]. The realization of Quantum Turbulence (QT) in atomic superfuids [8] creates the opportunity to investigate the behavior of a free-expanding speckle matter wave and its statistical properties. In a recent experiment, an atomic speckle was produced using multimode guided atomic beam [9] and was studied by measuring the temporal second-order correlation function $C^{(2)}(\tau)$. Here, the spatial second-order correlation function $C^{(2)}(\Delta r)$ is measured for the free-expanding atomic speckle. In this Letter, we use the correlation function to discuss in details the chaotic behavior of the speckle many-vortex condensate as it freely expands and compare the behavior of this turbulent atomic superfluid cloud in expansion with the propagation of a speckle light field. Our results clearly demonstrate that even in the chaotic regime, matter and light waves behave similarly. This finding, adds a new dimension to the matter-wave equivalence at the small scales world.

We first clarify a question of nomenclature: "Quantum Turbulence", which we use to characterize the turbulent BEC (TBEC), is loosely used by us in several of previous publications and in the current paper. It is to be understood as a short-hand version of "Turbulence in the Collective Response of Quantum Systems", which we believe to be unique to a Bose-Einstein condensate, as collective excitations are predominantly *ordered* phenomena: to cite a few, the dipole resonance in mixed BEC (two types of atoms with different masses), plasmon resonances in metal clusters, and giant resonances in nuclei. Even in a gently rotated BEC, vortex formation may increase to the point of forming an Abrikasov Lattice in a BEC [10–12], a highly ordered structure. The description of these ordered structures of vortices is the cranked Gross-Pitaevskii equation. In turbulent BEC, the vortices are formed in a disordered fashion and the resulting collective response is chaotic.

Our experimental apparatus consists in a BEC of ^{87}Rb atoms confined in a magnetic QUIC (QUadrupole-Ioffe Configuration) trap. The trap potential is characterized by an axial frequency $\omega_x = 2\pi \times 21.1(1)$Hz and a radial frequency $\omega_r = 2\pi \times 188.2(3)$Hz. The BEC sample contains 1.4×10^5 atoms with a small thermal fraction ($T = 170$ nK $\approx 0.47 T_C$). To perturb the BEC, a temporal oscillatory magnetic field is superimposed on the static QUIC trapping field. This extra field is produced by a fixed pair of anti-Helmholtz coils whose center is displaced (≈ 8 mm) from the QUIC trap minimum and its axis is tilted in a small angle ($\approx 5°$) from the trap major axis [8]. The oscillatory field is turned on during 31.7 ms (6 full cycles of excitation) at a frequency of 189 Hz. After the excitation stage, we let the perturbed atomic cloud evolve in-trap during 35 ms. Then, the condensate is released from the trap, expanding freely in time-of-flight (TOF) and a standard absorption image is performed to obtain the atomic cloud picture. For excitation amplitude higher than 350 mG/cm a quantum turbulence state was observed in the BEC. The momen-

tum distribution and collective modes of this clouds was already investigated in previous works [13].

The qualitative and quantitative characterization of the generated atomic QT has been analyzed in several previous publications [14, and references therein]. Briefly, the quantum gas emerges from this excitation either with the presence of scissors mode or with the nucleation of vortices, resulting from the interaction of the BEC with the thermal gas, and their further number proliferation along several directions. After a critical number of formed vortices, the system evolves into a tangle configuration characterizing the emergence of turbulence. Further excitation of the turbulent cloud by the external field results in a granulation state which corresponds to condensate grains surrounded by non-condensed atoms.

A typical result for the free expansion of the turbulent and non-turbulent clouds are shown in Fig. 1, where the cloud dimensions are plotted as a function of the time-of-flight. For a standard BEC expansion, Fig. 1(a), the aspect ratio inversion occurs at the crossing point, around the time-of-flight 8.5 ms. On the other hand, the turbulent cloud expands without any intersection point during the considered TOF interval, Fig. 1(b). The turbulent cloud indicates an almost self-similar type expansion with a shape and an aspect ratio nearly constant during the TOF. The vortex angular momentum reduces the cloud radius expansion rates and the almost self-similar expansion of a turbulent cloud has been explored as an evidence of turbulence in BEC [14]. At this point we mention that several other papers have addressed different questions related to the statistical properties of interacting many-body systems [15–18], and of an expanding cloud of BEC [19–21]. From figures 1(a) and 1(b) the expansion velocities in both cases are $\dot{R}_y = 3.9(1)$ μm/ms, $\dot{R}_x = 0.47(1)$ μm/ms for the regular BEC and $\dot{R}_y = 5.3(2)$ μm/ms, $\dot{R}_x = 1.5(1)$ μm/ms for the turbulent cloud, showing that the disordered matter-wave expands faster than the coherent one. Figures 1(c) and 1(d) show a sequence for the expansion of the regular BEC and turbulent cloud, respectively, for different TOF values. In Fig. 1(d) it is observed that topological defects, typical of a turbulent cloud, only appears in the 2D absorption image for sufficiently dilute samples. This condition imposes a lower limit on the TOF which may be used to probe experimentally this fine-grained structure.

Next we evaluate the density-density correlation function for the expanded matter wave and compare it with that of the speckle field, whose coherence, or lack of it can be described by the intensity-intensity correlation function, as was originally formulated by Hanbury-Brown-Twiss, in their quest for the determination of the sizes of astronomical objects [22].

The density as a function of r is simply the sum, $\rho(r) = \sum_i |\psi_i(r)|^2$, where $\psi_i(r)$ is the single particle wave function of the i-th atom at r. When vortices are

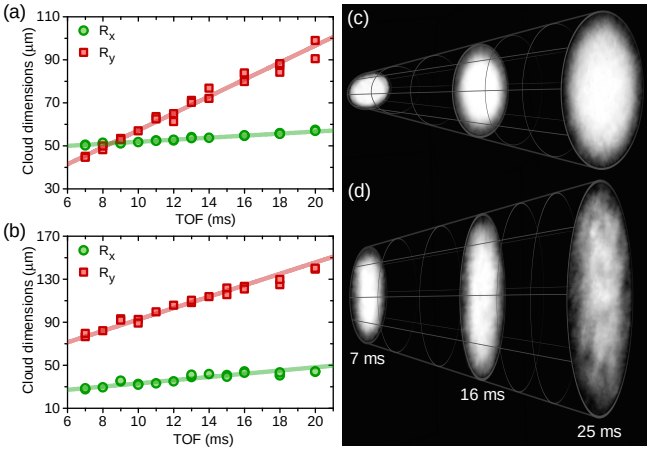

FIG. 1. (color online) Cloud expansion during time-of-flight. (a), (b) Cloud dimensions along the x and y directions, R_x and R_y, as a function of the time-of-flight for a regular BEC and a turbulent BEC, respectively. (c), (d) Sequence of three different time-of-flight showing the expansion of a regular BEC and a turbulent BEC, respectively.

present, the sum above is expanded to include the oscillatory component which counts the vortices. Therefore, the density function contains fluctuations due to the vortices present in the turbulent BEC, and it is convenient to extract from $\rho(r)$ an average component and a fluctuation, chaotic component, *viz*

$$\rho(r) = \langle \rho(r) \rangle + \rho_{fl}(r). \tag{1}$$

The average of $\rho_{fl}(r)$ is *by definition*, zero, $\langle \rho_{fl}(\mathbf{r}) \rangle = 0$. This property allows the calculation of the density-density correlation function of interest in the analysis of turbulent BEC as

$$C^{(2)}(r - r') = \frac{\langle \rho(r)\ \rho(r') \rangle}{\langle \rho(r) \rangle\ \langle \rho(r') \rangle} - 1 = \frac{\langle \rho_{fl}(r)\ \rho_{fl}(r') \rangle}{\langle \rho(r) \rangle\ \langle \rho(r') \rangle}. \tag{2}$$

The average density $\langle \rho(r) \rangle$, associated with the regular BEC without vortices, supplies a correlation function, Eq. (2), which is zero by definition. Correlation functions of amplitudes such as those encountered in the conductance of electrons in chaotic systems are calculated using Radom Matrix Theory (RMT). Recently these correlation functions were calculated and discussed in the case of Chaotic Quantum Dots, d = 1 mesoscopic devises containing a few electrons confined within a small region on the surface of normal material and on a graphene surface [23, 24]. In TBEC, RMT can also be applied in the case of other observables connected to the mobility of the vortices. More work needs to be done on these issues.

As regards the fluctuating density, $\rho_{fl}(r)$, the probability distribution, $P(\rho_{fl})$, is expected to be a normalized Gaussian, a consequence of the Central Limit Theorem. Thus $P(\rho_{fl}) = N \exp\left[-(\rho_{fl})^2/2\sigma^2\right]$, where σ^2 is the variance of the distribution, $\sigma^2 = \langle (\rho_{fl})^2 \rangle$, and N

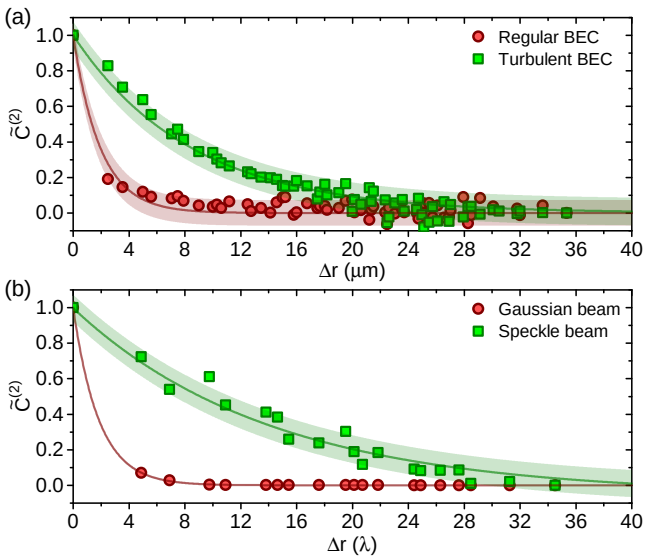

FIG. 2. (color online) Normalized correlation function, $\widetilde{C}^{(2)}(\Delta r)$. (a) for a regular BEC (red) and a turbulent cloud (green) as a function Δr. (b) for the numerical simulations of the a Gaussian (red) and a speckle beam of light (green) as a function of Δr, in units of λ, at a propagation distance where the Gaussian beam aspect ratio matches with the regular BEC of (a). The $\widetilde{C}^{(2)}(\Delta r)$ for a regular BEC (Gaussian beam) is zero except for very small Δr, whereas for a turbulent cloud (speckle beam) it has an exponential decay with a correlation length of $\ell_{Turb} = 8.5(2)$ μm ($\ell_{Speckle} = 13.8(8)\lambda$). The cloud dimensions are $R_x = 63(3)$ μm and $R_y = 198(6)$ μm and the beam waists are $w_x = 1876\lambda$ and $w_y = 2528\lambda$, showing that the correlation length is much shorter than the cloud (beam) sizes. The colored regions are confidence bands of the exponential decay fitting.

is the normalization constant, $N = \sqrt{2/\pi}/\sigma$. The variance is basically the correlation function at $\Delta r = 0$. It is convenient to present our result for the correlation function normalized to the variance, such that at $\Delta r = 0$ the correlation function is unity. In this way, we define the normalized correlation function as $\widetilde{C}^{(2)}(\Delta r) = C^{(2)}(\Delta r)/C^{(2)}(0)$. Of course in order to calculate averages such as $\langle \rho_{fl}(r)\rho_{fl}(r')\rangle$, one needs the functional r-dependence of $\rho_{fl}(r)$. Not having this at hand, we merely construct the average through sampling different values of Δr, and then performing the average as $\sum_{i=1}^{M} \rho_{fl}(r_i)\rho_{fl}(r_i')/M$. The large Δr behavior of the correlation function is expected to be a Gaussian or an exponential. In our analysis to follow the exponential decay with increasing Δr was found to better represent the behavior of the data, and the correlation length can be extracted by using $\widetilde{C}^{(2)}(\ell) = 1/e$. In the following we analyze the correlation function using the observed density, $\rho(r)$.

In Fig. 2(a), we analyze the normalized correlation function $\widetilde{C}^{(2)}(\Delta r)$ for a regular BEC and a turbulent cloud at 30 ms of time-of-flight. The correlation for a

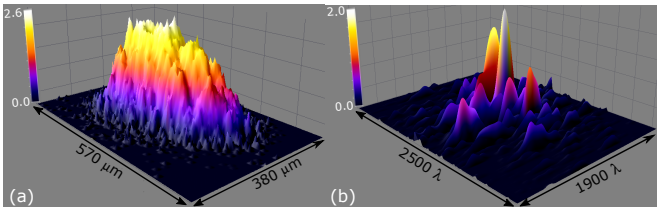

FIG. 3. (color online) Comparison between turbulent cloud and speckle beam. (a) Column integrated density profile for a turbulent BEC. (b)Intensity profile for the cross section of a speckle beam. The integration in one of the 3D dimension of the BEC cloud result in slight reducing the amplitude of density variations.

regular BEC is basically constant and close to zero. At short distances, $\widetilde{C}^{(2)}(\Delta r)$ is greater than zero due to the small thermal fluctuations originated from the thermal atoms component of the sample. The turbulent cloud shows a typical $\widetilde{C}^{(2)}(\Delta r)$ of a normalized decaying form at larger Δr, which is a result of a much shorter correlation length ($\ell_{Turb} = 8.5(2)$ μm) than the sizes of the cloud ($R_x = 63(3)$ μm and $R_y = 198(6)$ μm) and indicates the presence of fluctuations at smaller scales. The in-trap correlation length can be extracted from the TOF correlation length by $\ell^0_{Turb} = \ell_{Turb}/\sqrt{1+(\omega_r t)^2} \approx 1.3\xi$ [1], where t is the TOF and $\xi = 0.18$ μm is the BEC healing length, which is the typical vortex radius. The correlation length can well be associated with the event horizon radius of a single vortex, indicating clearly that the chaotic dynamics of TBEC is entirely connected to the vortices created in the disturbed BEC. While in speckle optics the correlation length is dependent on the scattering size, density of speckle centers, propagation time and wavelength, for the turbulent BEC it is a function of the vortex size, density of vortex, expansion time and de Broglie wavelength.

Such a behavior strongly reminds us of a speckle light field and allows us to establish an analogy between the light field and the expanding quantum gas. Indeed, a speckle field arises from a sum of complex statistically independent amplitudes bearing a random magnitude and phase [25]. For this purpose, we simulated a propagating coherent Gaussian beam and speckle light beam and compare with the expanding BEC and TBEC [26]. In Fig. 2(b), we present the normalized correlation function $\widetilde{C}^{(2)}(\Delta r)$ for the Gaussian and the speckle beam at a propagation distance where the Gaussian beam aspect ratio matches with the regular BEC of Fig. 2(a). The same decaying correlation function behavior is found for light field and the quantum gas. In Fig. 3, we present the atomic density absorption profile of an expanding turbulent cloud together with the cross section intensity profile of a propagating speckle field, showing the similarities between the distribution of the spatial fluctuations amplitudes.

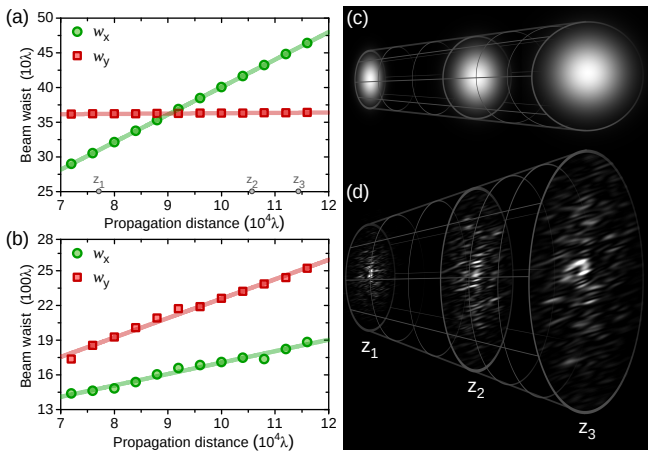

FIG. 4. (color online) Optical beam propagation. (a), (b) Beam sizes along the x and y directions, w_x and w_y, as a function of the propagation distance for a coherent Gaussian beam and a speckle beam, respectively. In the marked propagation distances z_1, z_2 and z_3, the Gaussian beam aspect ratio matches with the regular BEC at the three TOFs of Fig. 1(c). (c), (d) Sequence of three different propagation distances showing the expansion of a Gaussian beam and a speckle beam, respectively.

As is well known a coherent elliptical Gaussian laser beam presents an inversion of its aspect ratio during the propagation, this is equivalent to the aspect ratio inversion of coherent matter waves in a BEC. If we now consider the same elliptical beam, but with a speckle pattern on it, the divergence is quite different. The divergence angle for each direction is given by $\tan\theta_i = \lambda/\ell_i$, where ℓ_i is the correlation length of the speckle in the i-direction. For an isotropic speckle field the correlation length is equal in both directions, thus the beam divergence is the same for both directions. Therefore, the propagation takes place without inverting the aspect ratio, which tends to unity at very large distances (far-field regime). In Fig. 4 are presented the beam waists of the coherent Gaussian beam and the speckle beam, as a function of the propagation distance. The coherent and incoherent optical beams, of identical initial elliptical cross-section, follow distinct evolution due to the presence of disorder in the latter.

For the coherent beam, Fig. 4(a), inversion occur after a given propagation distance away from the focus. In contrast, for the speckle field, Fig. 4(b), the beam propagates in an almost self-similar shape, and the cross-section along each dimension increases faster when compared with the coherent beam case. That occurs when $\ell_i < w_i$, i.e. for a beam with many speckle grains, having a divergence angle larger for the case of speckle. From figures 4(a) and 4(b) the beam divergence in both cases are $\dot{w}_x = 39.64(2)\times10^{-3}$, $\dot{w}_y = 0.48(1)\times10^{-3}$ for the coherent Gaussian beam and $\dot{w}_x = 0.098(5)$ and $\dot{w}_y = 0.167(6)$ for the speckle beam, showing that the disordered light-wave expands faster than the coherent one, similar to the quantum gas case (see Fig. 1). Figures 4(c) and 4(d) show a sequence for the propagation of the coherent Gaussian and speckle beams, respectively. Those properties allow a comparison between Fig. 1 and 4 showing the equivalence between the propagating speckle light field and the expansion of the corresponding matter wave originated from a turbulent cloud.

An important point concerning our measurements is that they are obtained from the cloud absorption image. This corresponds to a projection of the cloud atomic density distribution onto a two dimensional plane. Despite the fact that this procedure smooths the amplitude of the fluctuations (as shown in Fig. 3), the correlation length measured after projection is the same as in three dimensions. We support this claim by simulating a 2D optical speckle beam and its projection in one dimension. We observe that the effect on the correlation length, extracted from $\widetilde{C}^{(2)}(\Delta r)$, remains unaffected [26].

The introduction of disorder in matter waves, which can be done through the emergence of turbulence in an atomic cloud, opens up a large new window of research opportunities to better understand the nature of the disorder in the quantum world. It may provide further insight into the statistical behavior of quantum turbulence and the probability distribution of the density of the vortices which represent the microscopic "constituents" of the turbulent gas. The different slopes seen in Fig. 1(b) could be used to study the anisotropy of turbulence in atomic superfluid.

In conclusion, we have supplied a detailed analysis of the chaotic nature of a turbulent condensate, and presented evidence that the correlation length is intimately related to the size of a single vortex. We have shown that the average density of the turbulent BEC is close to the density of the regular BEC. We further demonstrated the equivalence between a turbulent atomic superfluid in expansion with a speckle light field propagation. This finding would allow further mapping of both phenomena on each other as well as adds further understanding of the statistics of matter waves. The measurement of second-order correlation function can be an alternative method to obtain the first-order correlation function using the well established Siegert relation [27]. Speckle like behavior in turbulent quantum fluids consists of a three dimensional speckle field and may be an excellent candidate to explore important aspect of structures and the tomography of speckle fields in three dimensions.

We thank FAPESP, CAPES and CNPq (project PVE 400228/2014-9) for financial support. We greatly appreciate collaboration with P. Courteille (IFSC), E. Henn (IFSC) and G. Roati (LENS/Italy). MSH also acknowledges a Senior Visiting Professorship granted by CAPES (program CAPES/ITA-PVS).

* pedro.ernesto.tavares@usp.br

[1] Y. Castin and R. Dum, Phys. Rev. Lett. **77**, 5315 (1996).

[2] F. Impens and C. J. Bordé, Phys. Rev. A **79**, 043613 (2009).

[3] J. F. Riou, Y. Le Coq, F. Impens, W. Guerin, C. J. Bordé, A. Aspect, and P. Bouyer, Phys. Rev. A **77**, 033630 (2008).

[4] Y. Le Coq, J. H. Thywissen, S. A. Rangwala, F. Gerbier, S. Richard, G. Delannoy, P. Bouyer, and A. Aspect, Phys. Rev. Lett. **87**, 170403 (2001).

[5] T. Busch, M. Köhl, T. Esslinger, and K. Mølmer, Phys. Rev. A **65**, 043615 (2002).

[6] J. F. Riou, W. Guerin, Y. Le Coq, M. Fauquembergue, V. Josse, P. Bouyer, and A. Aspect, Phys. Rev. Lett. **96**, 070404 (2006).

[7] A. Couvert, M. Jeppesen, T. Kawalec, G. Reinaudi, R. Mathevet, and D. Guéry-Odelin, Europhys. Lett. **83**, 50001 (2008).

[8] E. A. L. Henn, J. A. Seman, G. Roati, K. M. F. Magalhães, and V. S. Bagnato, Phys. Rev. Lett. **103**, 045301 (2009).

[9] R. G. Dall, S. S. Hodgman, A. G. Manning, M. T. Johnsson, K. G. H. Baldwin, and A. G. Truscott, Nat. Comm. **2**, 291 (2011).

[10] M. S. Hussein and O. K. Vorov, Annals of Physics **298**, 248 (2002).

[11] O. K. Vorov, M. S. Hussein, and P. V. Isacker, Phys. Rev. Lett. **90**, 200402 (2003).

[12] O. K. Vorov, P. Van Isacker, M. S. Hussein, and K. Bartschat, Phys. Rev. Lett. **95**, 230406 (2005).

[13] K. J. Thompson, G. G. Bagnato, G. D. Telles, M. A. Caracanhas, F. E. A. dos Santos, and V. S. Bagnato, Laser Phys. Lett. **11**, 015501 (2014); A. Bahrami, P. Tavares, A. Fritsch, Y. Tonin, G. Telles, V. Bagnato, and E. Henn, J. Low Temp. Phys. **180**, 126 (2015); A. R. Fritsch, P. E. S. Tavares, A. Bahrami, Y. R. Tonin, E. A. L. Henn, V. S. Bagnato, and G. D. Telles, J. Low Temp. Phys. **180**, 144 (2015).

[14] M. C. Tsatsos, P. E. S. Tavares, A. Cidrim, A. R. Fritsch, M. A. Caracanhas, F. E. A. dos Santos, C. F. Barenghi, and V. S. Bagnato, Physics Reports **622**, 1 (2016).

[15] Z. Hadzibabic, P. Krüger, M. Cheneau, B. Battelier, and J. Dalibard, Nature **441**, 1118 (2006).

[16] S. Hofferberth, I. Lesanovsky, T. Schumm, A. Imambekov, V. Gritsev, E. Demler, and J. Schmiedmayer, Nature Physics **4**, 489 (2008).

[17] Z. Hadzibabic, Nature Physics **6**, 643 (2010).

[18] A. L. Gaunt, R. J. Fletcher, R. P. Smith, and Z. Hadzibabic, Nature Physics **9**, 271 (2013).

[19] S. Burger, K. Bongs, S. Dettmer, W. Ertmer, K. Sengstock, A. Sanpera, G. V. Shlyapnikov, and M. Lewenstein, Phys. Rev. Lett. **83**, 5198 (1999).

[20] S. Dettmer, D. Hellweg, P. Ryytty, J. J. Arlt, W. Ertmer, K. Sengstock, D. S. Petrov, G. V. Shlyapnikov, H. Kreutzmann, L. Santos, and M. Lewenstein, Phys. Rev. Lett. **87**, 160406 (2001).

[21] D. Hellweg, L. Cacciapuoti, M. Kottke, T. Schulte, K. Sengstock, W. Ertmer, and J. J. Arlt, Phys. Rev. Lett. **91**, 010406 (2003).

[22] R. Hanbury-Brown and R. Q. Twiss, Nature , 27 (1956).

[23] J. G. G. S. Ramos, A. L. R. Barbosa, B. V. Carlson, T. Frederico, and M. S. Hussein, Phys. Rev. E **93**, 012210 (2016).

[24] J. G. G. S. Ramos, M. S. Hussein, and A. L. R. Barbosa, Phys. Rev. B **93**, 125136 (2016).

[25] J. W. Goodman, *Speckle Phenomena in Optics: Theory and Applications* (Roberts & Company, 2010).

[26] See Supplemental Material for the experimental details, the description of optical speckle simulations and the effect of the projection onto the second-order correlation function.

[27] J. W. Goodman, *Statistical Optics* (John Wiley & Sons, 2000).